Structural Damage Condition of Buildings with a Sparse Number of Sensors Using Machine Learning: Case Study

Edisson Alberto Moscoso Alcantara(✉) and Taiki Saito

Toyohashi University of Technology, Toyohashi 441-8580, Aichi, Japan
moscoso.alcantara.edisson.alberto.eh@tut.jp

Abstract. The optimum location of signal sensors in actual buildings to determine the structural damage condition using machine learning is discussed in this study. The target buildings are a local government office and a Fire Station in Japan, with two acceleration sensors located on the ground and the roof level of the buildings. An additional sensor location is considered in this study. The structural damage condition is evaluated by machine learning (ML) methods from the sensor signals for five cases of single and multiple sensor locations. The maximum story drift is used as an identifier of the structural damage condition. Seven ML methods are developed, and their accuracy is compared. Several intensity measures (IM) obtained from each sensor signal are used as input features for the ML models, and the prediction importance level of each IM is evaluated in order to establish its usefulness. Finally, the results are compared to the methodology using wavelet power spectrum and convolutional neural network to predict the damage condition of buildings.

Keywords: Damage condition · Machine learning · Monitored buildings · Sparse number of sensors · Structural Health Monitoring

1 Introduction

Currently, seismic instrumentation by acceleration sensors is used worldwide because it allows for characterizing the structure's performance before, during, and after an earthquake occurrence. For example, according to earthquake-resistance design standards, a minimum of 12 sensors are required for buildings with a number of stories from 6 to 10 above the ground for evaluating all structural directions [1, 2]. However, researchers have developed methodologies with a sparse number of sensors to predict the performance of buildings immediately after an earthquake occurs. For instance, Xu and Mita [3] presented a method that estimates the maximum story drift ratio and time histories of the relative story displacements of buildings using one acceleration sensor on the roof level. Besides, Moscoso and Saito [4] proposed a methodology to identify the damage condition of structures based on the Convolutional Neural Network (CNN) method using wavelet power spectrum (WPS) from the acceleration signal of a sensor on the top floor. Also, studies on optimal sensor placement for damage detection were developed by researchers [5–7].

A. Ilki et al. (Eds.): *fib* Symposium 2023, LNCE 350, pp. 128–140, 2023.
https://doi.org/10.1007/978-3-031-32511-3_15

This study presents a methodology to obtain the structural damage condition of buildings (represented by the maximum story drift ratio) and the optimum location of a sparse number of sensors using Intensity Measures (IMs) and Machine Learning (ML) methods. The IMs represent the structural characteristic of signals based on acceleration, velocity, displacement, or a combination among them (hybrid) [8]. They are obtained from the sensor's signals and used as features for training seven ML models. In order to establish the optimum ML method and sensor's location, the accuracy and dispersion (represented by the determination coefficient and the standard deviation of the maximum story drift ratios) are compared by applying them to the Tahara City Hall and Toyohashi Fire Station buildings (target buildings). Also, the results are compared to the methodology using wavelet power spectra and the convolutional neural network method to predict the damage condition [4].

2 Research Methodology

This research studies three sensor locations: Ground, Roof floor, and Rooftop sensor locations, as defined in Fig. 1.

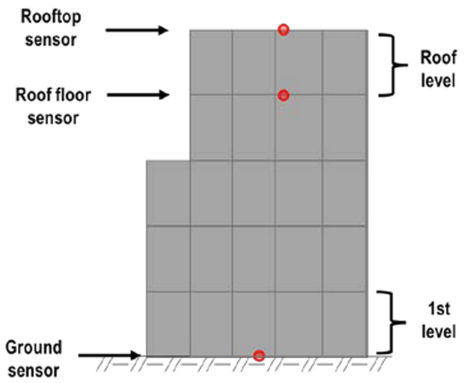

Fig. 1. Definition of the sensor's location on the target building.

From the location of the sensors, five cases are studied for the target buildings (Table 1):

The procedure to obtain the damage condition of buildings is as follows and its scheme is shown in Fig. 2:

1. Obtain the signal acceleration by the sensors.
2. Obtain the Intensity Measures.
3. Use the IMs as features for the ML models.
4. Predict the maximum story drift ratio with the ML models.
5. Classify the predicted maximum story drift ratio to obtain the damage condition of the building.

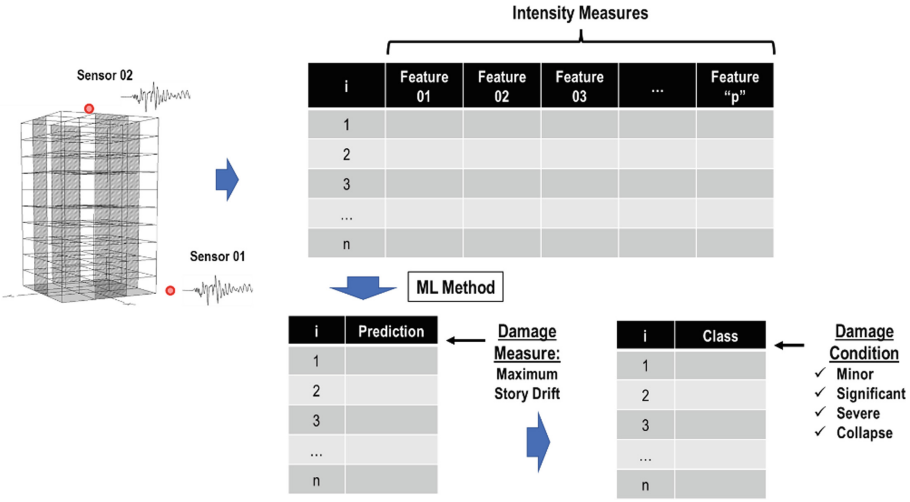

Fig. 2. Procedure scheme of the study.

Table 1. Sensor location cases.

Abbreviation	Case according to the sensor location usability
G	Only using the Ground sensor
RF	Only using the Roof floor sensor
Rt	Only using the Rooftop sensor
G + RF	Using the Ground and Roof floor sensor
G + Rt	Using the Ground and Rooftop sensor

3 Intensity Measures (IMs)

The IMs can be obtained based on either acceleration (A), velocity (V), displacement (D), or combining them (H: hybrid IM). They have been studied over the years to characterize the structural building responses using only the ground motion acceleration [9]. Table 2 shows the IMs used in this study.

Since the acceleration sensors were considered in this study, the double integration process was used to obtain the velocity and displacement signals.

Table 2. Intensity Measures

N°	Name	Abbreviation	Based on	Definition	Reference
1	Peak Ground Acceleration	PGA	A	$PGA = \max_{0 \le t \le t_f} \lvert \ddot{u} \rvert$	[10]
2	5% damped first-mode Spectral Acceleration	$Sa(T_1, 5\%)$	A	$S_a(T_1, 5\%) = \lvert max(\ddot{u}_{(T_1,5\%)} + \ddot{u}_g) \rvert$	[10, 11]
3	Average Spectral Acceleration	Sa_{avg}	A	$Sa_{avg} = \left(\prod_{t=1}^{n} S_{a(T_i)} \right)^{\frac{1}{n}}$	[12]
4	Effective Peak Acceleration	EPA	A	$EPA = \frac{1}{2.5} * \int_{0.1}^{0.5} S_{a(T,h=5\%)} dT$	[13]
5	SR Power-law form IM	IM_{SR}	A	$IM_{SR} = S_a(T_1)^{1-\alpha} S_a\left(\sqrt{R}T_1\right)^{\alpha}$	[14]
6	CR Power-law form IM	IM_{CR}	A	$IM_{CR} = S_a(T_1)^{1-\alpha} S_a\left(\sqrt[3]{R}T_1\right)^{\alpha}$	[14]
7	Earthquake Power Index	EPI	A	$EPI = \frac{1}{t} * \int_0^t {a_{(\tau)}}^2 d\tau$	[15]
8	Root Mean Square Acc	RMS	A	$RMS = \sqrt{EPI}$	[15]
9	Bojórquez & Iervolino IM	I_{Np}	A	$I_{N_P} = S_a(T_1, 5\%) \cdot \left(\frac{Sa_{avg}}{S_a(T_1,5\%)} \right)^{\alpha}$	[16]
10	Arias Intensity	AI	A	$AI = \frac{\pi}{2g} * \int_0^t {a_{(\tau)}}^2 d\tau$	[17]
11	Sarma & Yang IM	A_{95}	A	$A_{95} = 0.05 \cdot \int_0^t {a_{(\tau)}}^2 d\tau$	[18]
12	Characteristic Intensity	I_C	A	$I_c = RMS^{1.5} \cdot t95\_t05^{0.5}$	[19]
13	Riddell & Garcia Acceleration IM	Ia	A	$I_a = a_{max} \cdot t95\_t05^{1/3}$	[20]
14	Cumulative Absolute Velocity	CAV	A	$CAV = \int_0^t \lvert a_{(\tau)} \rvert d\tau$	[21]

(*continued*)

Table 2. (*continued*)

N°	Name	Abbreviation	Based on	Definition	Reference
15	Standardized Cumulative Absolute Velocity	S-CAV	A	$S-CAV = \sum_{t=1}^{N}\left(H_{(PGA_i-0.025)}\int_{i-1}^{i}\lvert a(t)\rvert dt\right)$	[22]
16	Two-parameter hazard IM	TPH	A	$R_{S_a} = S_a(T_f)\big/ S_a(T_1)$ $TPH = S_a(T_1)\cdot R_{S_a}^{\alpha}$	[23]
17	Peak Ground Velocity	PGV	V	$PGV = \underset{0\le t\le t_f}{max}\lvert v_{(t)}\rvert$	[10, 24]
18	Squared Velocity	V_{sq}	V	$V_{sq} = \int_0^t {v_{(\tau)}}^2 d\tau$	[8]
19	Root Squared Velocity	V_{rms}	V	$V_{rms} = \sqrt{V_{sq}}$	[8]
20	Fajfar et al. IM	I_F	V	$I_F = PGV\cdot t95\_t05^{0.25}$	[25]
21	Riddell & Garcia Velocity IM	I_v	V	$I_v = PGV^{2/3}\cdot t95\_t05^{1/3}$	[20]
22	5% damped first-mode Spectral Velocity	Sv(T1, 5%)	V	$S_v(T_1, 5\%) = S_{v(T_1,h)}$	[10, 11]
23	Housner Spectrum Intensity	SI_H	V	$SI_H = \int_{0.1}^{2.5} S_V d\tau$	[26]
24	Peak Ground Disp.	PGD	D	$PGD = \underset{0\le t\le t_f}{max}\lvert u_{(t)}\rvert$	[10]
25	5% damped first-mode Spectral Displacement	Sd(T1, 5%)	D	$S_d(T_1, 5\%) = S_{d(T_1,h)}$	[10, 11]
26	Riddell & Garcia Velocity IM	I_d	D	$I_d = PGD\cdot t95\_t05^{1/3}$	[20]
27	Cosenza & Manfredi IM	Iz	H	$I_Z = \int_0^t a_{(t)}^2 dt \Big/ (PGA\cdot PGV)$	[27]

4 Machine Learning Methods

The following seven ML methods are used, and their hyperparameters are calibrated after several runnings (training process) in order to optimize the prediction. The optimum IMs for predicting are obtained from feature importance level (from 0 to 1), which was obtained using the Gini importance technique [28, 29] of the regression tree methods (no for Linear regression and Multilayer perception).

(a) Linear Regression

This linear model method assumes the output (prediction) is linearly dependent on the features. The coefficients (weights) are updated in order to minimize the prediction error obtained from the reference and predicted values. [30, 31].

(b) Decision Tree

This method builds the best decision-making tree by splitting and selecting the order of the roots and leaves. The leaves are chosen when it is not possible for more optimization below those nodes. [32, 33].

(c) Random Forest

This method builds several decision trees (forest) from bootstrapped datasets (a new random dataset with the same size as the original one), increasing its accuracy in this way. The new data to predict is evaluated in the forest. [28, 34].

(d) Gradient Boosting (Gradient Boost)

This method makes a tree to obtain residuals instead of predictions. Then, a new predictor is built using the previous predictor (the first one predicts the same value for all and then is updated) and adds the residuals predictor (a learning rate scales it). Therefore, the new predictor is based on the previous tree's errors. [28].

(e) AdaBoost

This method fits a regressor on the original dataset. Then it fits additional copies of the regressor on the same dataset, but the weights of instances are adjusted according to the error of the current prediction. [28].

(f) Extreme Gradient Boosting (XGBoost)

This ML method is called extreme because it is built with several parts. Like Gradient Boost, the regression tree is obtained using residuals instead of predictions by the similarities and gain values method for splitting and getting the thresholds. The pruning method is used to reduce this tree. Also, this method uses the Regularization parameter to minimize the prediction's sensitivity to individual observations. Finally, it uses the original previous predictor and learning rate to obtain a new predictor. [35].

(g) Multilayer Perceptron

It interconnects a group of perceptrons and transmits data to others inspired by the biological neural networks that constitute animal brains. Each connection has weights that are adjusted to reduce the error. [32, 36].

5 Case Study

5.1 Target Buildings

The Tahara City Hall (TCH) and Toyohashi Fire Station (TFS) buildings located in Japan are studied in this research (shown in Fig. 3 and Fig. 4, respectively). They are instrumented with two sensors in G and the RF locations. However, this research also evaluates the case of the sensor on the rooftop (Rt location).

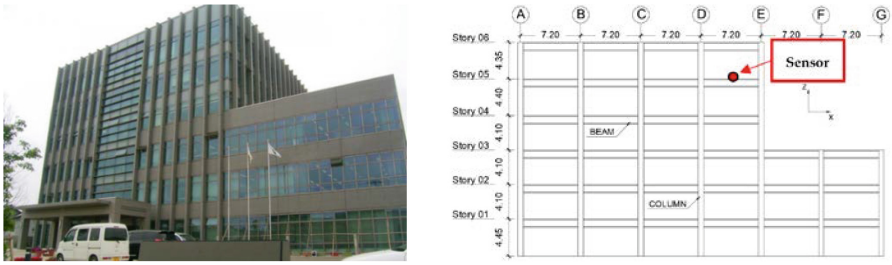

(a) (b)

Fig. 3. (a) Tahara City Hall building. (b) Elevation drawing view.[4]

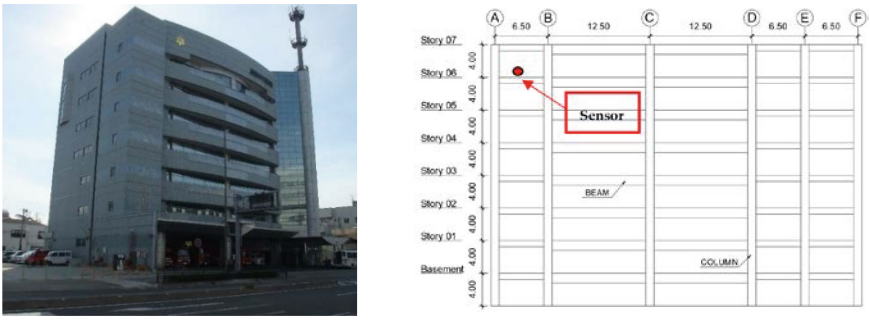

(a) (b)

Fig. 4. (a) Toyohashi Fire Station Building. (b) Elevation drawing view. [4]

5.2 Structural Model

The buildings are modeled by the STERA_3D software developed by one of the authors as follows [4]:

– Three-dimensional frame models are carried out.
– The elastic and inelastic behavior of their members is as follows:

- For the beams, nonlinear flexural springs are used at both ends of the member. Degrading trilinear slip and bilinear hysteretic models are considered for RC and steel sections, respectively.

- For the columns, nonlinear multi-spring cross-section models are used at both ends of the member in order to consider the bidirectional-flexural and axial effects. Bilinear hysteretic models are considered for steel (tension and compression) and concrete (only compression).
- A nonlinear shear spring is used in the middle of the beams and columns, and an origin-oriented poly-linear hysteretic model is considered.

– Only unidirectional nonlinear dynamic analysis is carried out.

5.3 Input Earthquake Ground Acceleration Records

A database of earthquake records was obtained from the Center for Engineering Strong Motion Data by USGS and the California Geological Survey [37]. In order to reduce the computation time of the structural analyses, 183 records were selected with a maximum of 3000 samples, a minimum PGA of 400 gal, and a time range from 5% to 95% of the Arias Intensity [4, 17].

5.4 Incremental Dynamic Analyses

The Incremental Dynamic Analysis (IDA) obtains the structural responses (maximum story drift ratio), increasing the ground motion intensity by a representative IM. The scale factors are selected in order to cover the elastic and inelastic behavior. The characteristics of the IDA are as follows:

– $Sa(T_1, 5\%)$ is used as IM for developing the incremental analysis [38].
– All the records were scaled in order to obtain the same $Sa(T_1, 5\%)$.
– The minimum, maximum and incremental steps of $Sa(T_1, 5\%)$ were 25, 2000, and 25 gal, respectively.
– Since the TCH building has an irregular structural configuration, the incremental step of $Sa(T_1, 5\%)$ over 250 gal was each 5 gal.

Therefore, 65 880 and 14 640 nonlinear time-history analyses were carried out for TCH and TFS buildings.

5.5 Structural Damage Condition of Buildings

The damage condition is obtained from Moscoso et al. [39] and shown in Table 3.

Since the collapse state is greater than 1/75 (0.0133), results greater than 0.02 were not considered in order to increase and reduce the accuracy and dispersion of the ML models, respectively.

Table 3. Structural damage condition.

Damage condition	Maximum story drift ratio
No damage	$<1/300$
Minor damage	$\geq 1/300$ but $<1/150$
Significant damage	$\geq 1/150$ but $<1/100$
Severe damage	$\geq 1/100$ but $<1/75$
Collapse	$\geq 1/75$

6 Data Analysis and Results of ML Methods

6.1 Training and Testing Process

For the training and testing process, 146 (80%) records and 37 (20%) new records were randomly selected, respectively. In order to increase the number of results for each ML model (to reduce a biased process), 50 random records selection were carried out. Therefore, 50 prediction results are obtained.

The prediction accuracy of the ML models is evaluated by the coefficient of determination (R^2) (an example result is shown in Fig. 5(a)). A normal distribution function of the R^2 from the 50 prediction results is assumed (see Fig. 5(b)). The maximum (Max.), mean, and standard deviation (σ) of the R2 are computed to compare the effectiveness and the dispersion among the ML models and sensor locations. Besides, the importance level of the features (IMs) for predicting is obtained for each case, as shown in Fig. 5(c).

6.2 ML Method Results

Table 4 and Table 5 show the best ML method results for the Tahara City Hall and Toyohashi Fire Station buildings. The IMs are ordered descending from left to right (collected from the feature importance levels greater than 0.05).

For the CNN method [4], only the maximum R^2 was obtained from Rt location, which is 0.825 and 0.909 for Tahara City Hall and Toyohashi Fire Station buildings, respectively. Notice that the Gradient Boosting method provides better results than the CNN method.

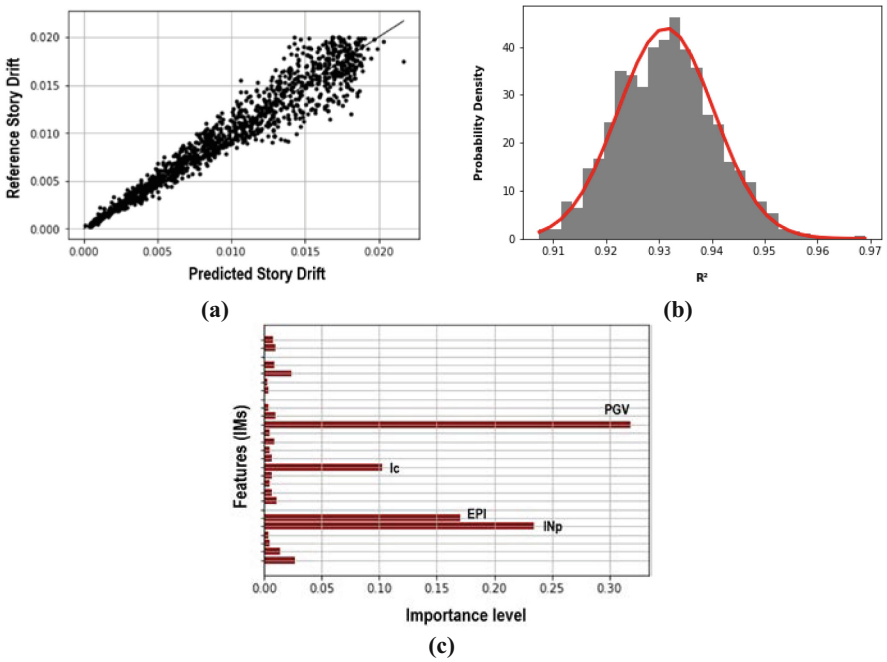

Fig. 5. Results example (a) Story drift prediction and reference ($R^2 = 0.94$). (b) Normal distribution function of the R^2 from the 50 records selection cases (mean = 0.931; $\sigma = 0.009$). (c) Importance levels of the features (IMs).

Table 4. Tahara City Hall building Results.

Sensor Location	Gradient Boost			
	Max	Mean	σ	IM
G	0.908	0.865	0.024	SaT1 / EPA
Rt	0.897	0.857	0.021	PGA / PGV
RF	0.904	0.845	0.031	PGA
G + Rt	0.926	0.892	0.021	G_SaT1 / R_PGA / R_EPA / G_INp
G + RF	0.914	0.875	0.02	R_PGA/G_SaT1

Table 5. Toyohashi Fire Station building Results.

Sensor Location	Gradient Boost			
	Max	Mean	σ	IM
G	0.915	0.873	0.022	SIH / EPA
Rt	0.951	0.931	0.009	PGV / PGA / RMS
RF	0.908	0.865	0.02	PGV / Ic/EPA / EPI / RMS / PGA
G + Rt	0.95	0.928	0.012	R_PGV / R_RMS / G_SaT1
G + RF	0.925	0.893	0.016	G_SIH/G_PGV/R_RMS

7 Conclusions and Discussion

In this research, a proposed methodology is proposed to obtain the structural damage condition of buildings and the optimum location of a sparse number of sensors using Intensity Measures and Machine Learning methods. This methodology is applied to two actual buildings, Tahara City Hall and Toyohashi Fire Station buildings, and the results are summarized as follows:

- For the Tahara City Hall building, the Gradient Boost is the ML method that gives the best maximum, mean, and σ of the R2 results, which are 0.926, 0.892, and 0.021, respectively. They are obtained using the G + Rt sensor location. They are greater than the given by the CNN method [4].
- For the Toyohashi Fire Station building, the Gradient Boost is the ML method that gives the optimum maximum, mean, and σ of the R^2 results, which are 0.951, 0.931, and 0.009, respectively. They are obtained using the Rt sensor location. They are greater than the given by the CNN method [4].
- The optimum sensor location is when the Ground and Rooftop sensors work simultaneously or only the Rooftop sensor.
- The acceleration intensity measures are the main features for predicting the Tahara City Hall building's damage condition.
- The velocity intensity measures are the main intensity measures for Toyohashi Fire Station.

Instrumental buildings can use this methodology for future earthquakes to define the best sensor's location and intensity measures for predicting their damage condition with high accuracy.

References

1. Akelyan MS et al (2020) An alternative procedure for seismic analysis and design of tall buildings located in the los angeles region 2020 edition. Los Angeles Tall Buildings Structural Design Council 2020
2. PEER Center (2010) Guidelines for performance-based seismic design of tall buildings; Pacific Earthquake Engineering Research Center, College of Engineering

3. Xu K, Mita A (2020) Estimation of maximum drift of MDOF shear structures using only one accelerometer. In: Materials Research Proceedings 2020, p 18
4. Moscoso Alcantara EA, Saito T (2022) Convolutional neural network-based rapid post-earthquake structural damage detection: case study. Sensors 22:6426
5. Capellari G, Chatzi E, Mariani S (2016) An optimal sensor placement method for SHM based on Bayesian experimental design and Polynomial Chaos Expansion. In: Proceedings of the ECCOMAS congress 2016 PROCEEDINGS, pp 6272–6282
6. Zhang J, Maes K, De Roeck G, Reynders E, Papadimitriou C, Lombaert G (2017) Optimal sensor placement for multi-setup modal analysis of structures. J Sound Vib 401:214–232
7. Tan Y, Zhang L (2020) Computational methodologies for optimal sensor placement in structural health monitoring: a review. Struct Health Monit 19:1287–1308
8. Buratti N (2012) A comparison of the performances of various ground–motion intensity measures. In: Proceedings of the Proceedings of the 15th world conference on earthquake engineering, Lisbon, Portugal, pp 24–28
9. Xu Y, Lu X, Tian Y, Huang Y (2020) Real-time seismic damage prediction and comparison of various ground motion intensity measures based on machine learning. J Earthq Eng, 1–21
10. Douglas J (2003) Earthquake ground motion estimation using strong-motion records: a review of equations for the estimation of peak ground acceleration and response spectral ordinates. Earth Sci Rev 61:43–104
11. Chopra AK (2007) Elastic response spectrum: a historical note. Earthquake Eng Struct Dynam 36:3–12
12. Baker JW, Allin Cornell C (2006) Spectral shape, epsilon and record selection. Earthquake Eng Struct Dynam 35:1077–1095
13. Newmark NM, Hall WJ (1982) Earthquake spectra and design. Engineering monographs on earthquake criteria
14. Mehanny SS (2009) A broad-range power-law form scalar-based seismic intensity measure. Eng Struct 31:1354–1368
15. Housner G (1975) Measures of severity of earthquake ground shaking. In: Proceedings of the Proceedings of US National Conference on Earthquake Engineering, p 6
16. Bojórquez E, Iervolino I (2011) Spectral shape proxies and nonlinear structural response. Soil Dyn Earthq Eng 31:996–1008
17. Arias A (1970) A measure of earthquake intensity. Seismic design for nuclear power plants. Massachusetts Institute of Technology
18. Sarma S, Yang K (1987) An evaluation of strong motion records and a new parameter A95. Earthq Eng Struct Dynam 15:119–132
19. Park Y-J, Ang AH-S, Wen YK (1985) Seismic damage analysis of reinforced concrete buildings. J Struct Eng 111:740–757
20. Riddell R, Garcia JE (2001) Hysteretic energy spectrum and damage control. Earthq Eng Struct Dynam 30:1791–1816
21. Reed JW, Kassawara RP (1990) A criterion for determining exceedance of the operating basis earthquake. Nucl Eng Des 123:387–396
22. Campbell KW, Bozorgnia Y (2011) Prediction equations for the standardized version of cumulative absolute velocity as adapted for use in the shutdown of US nuclear power plants. Nucl Eng Des 241:2558–2569
23. Cordova PP, Deierlein GG, Mehanny SS, Cornell CA (2000) Development of a two-parameter seismic intensity measure and probabilistic assessment procedure. In: Proceedings of the second US-Japan workshop on performance-based earthquake engineering methodology for reinforced concrete building structures, pp 187–206
24. Bommer JJ, Alarcon JE (2006) The prediction and use of peak ground velocity. J Earthquake Eng 10:1–31

25. Fajfar P, Vidic T, Fischinger M (1990) A measure of earthquake motion capacity to damage medium-period structures. Soil Dyn Earthq Eng 9:236–242
26. Housner GW (1952) Intensity of ground motion during strong earthquakes
27. Cosenza E, Manfredi G (1998) A seismic design method including damage effect. In: Proceedings of the 11th european conference on earthquake engineering, pp 6–11
28. Géron A (2022) Hands-on machine learning with Scikit-Learn, Keras, and TensorFlow, O'Reilly Media, Inc. Sebastopol
29. Bishop CM, Nasrabadi NM (2006) Pattern recognition and machine learning, vol 4. Springer, Heidelberg
30. Shalev-Shwartz S, Ben-David S (2014) Understanding machine learning: From theory to algorithms. Cambridge University Press, Cambridge
31. Su X, Yan X, Tsai CL (2012) Linear regression. Wiley Interdiscip Rev Comput Stat 4:275–294
32. Daumé, H (2017) A course in machine learning. Hal Daumé III
33. Myles AJ, Feudale RN, Liu Y, Woody NA, Brown SD (2004) An introduction to decision tree modeling. J Chemometrics J Chemometrics Soc 18:275–285
34. Biau G, Scornet E (2016) A random forest guided tour. TEST 25(2):197–227. https://doi.org/10.1007/s11749-016-0481-7
35. Chen T et al (2015) Xgboost: extreme gradient boosting. R package version 0.4-2, 1:1–4
36. Noriega L (2005) Multilayer perceptron tutorial. School of Computing. Staffordshire University, vol 4, p 5
37. Center for Engineering Strong Motion Data (CESMD). https://www.strongmotioncenter.org/. Accessed 1 Mar 2021
38. Shome N (1999) Probabilistic seismic demand analysis of nonlinear structures. Stanford University
39. Moscoso Alcantara EA, Bong MD, Saito T (2021) Structural response prediction for damage identification using wavelet spectra in convolutional neural network. Sensors 21:6795